Electronic Supplementary Information (ESI) for

Piezoelectric Induced Reversal Photocatalytic Performances for Carbon Nitride with Different Structures

Haoqing Zhang,[a] Zhonghui Xia,[a] Ping Niu[*,a], Xiaojuan Zhi,[a, b] Rui Dai,[b] Silin Chen,[b]

Shulan Wang[b] and Li Li[*,a]

[a] School of Metallurgy, Northeastern University, Shenyang 110819, P. R. China

[b] Department of Chemistry, College of Science, Northeastern University, Shenyang

110819, Liaoning, P. R. China.

* Corresponding authors:

Ping Niu. E-mail: niup@smm.neu.edu.cn

Li Li. E-mail: lilicmu@alumni.cmu.edu

Experimental Section

Materials:

Melamine ($C_3H_6N_6$) was purchased from Sinopharm Group Chemical Reagent Co., Ltd. Lithium chloride (LiCl) was purchased from Macklin. Potassium chloride (KCl) and sodium chloride (NaCl) were purchased from Tianjin Yongda Chemical Reagent Co., Ltd. All chemicals were of analytical grade and used without further purification. The water used in the whole experiment is deionized water.

Characterizations:

The XRD patterns were identified by X-ray diffraction (XRD, D8 Discover, Brook, USA) using Cu Kα radiation (acceleration voltage of 40 kV and current of 40 mA). The morphology of samples was recorded using the scanning electron microscope (SEM, Quanta250FEG, FEI Co., Ltd.) equipped with Oxford SDD energy spectrometer. The surface functional groups were characterized by IS20 modeled fourier transform infrared spectrometer (FT-IR, Thermo Fisher Scientific). The UV-vis absorption spectra were collected on JACSCO-500 spectrophotometer. The Brunauer-Emmett-Teller (BET) method was used to evaluate the specific surface area of the sample, and the pore size distribution was analyzed by non-local density functional theory (NLDFT) using an American micromeritics TriStar II 3020.3.02 analyzer under N_2 at 77 K. Steady-state fluorescence spectrometer (Fluoromax-4, HORIBA, LTD. Japan) was used to reveal the charge carrier behaviors and the excitation wavelength was 360 nm.

Finite element simulation

The stress responses of Melon, PHI and PTI under ultrasonic induced cavitation pressure were simulated by finite element method (ANSYS R19.2). 3×3×1 μm bulk, porous block and hollow tube were built using Auto CAD to roughly simulate the geometric characteristics of Melon, PHI and PTI. The impact force of ultrasonic induced cavitation bubble collapse on the sample is 108 Pa.[1] All material properties, divided grid and constrained surface were consistent, which makes the samples comparable.
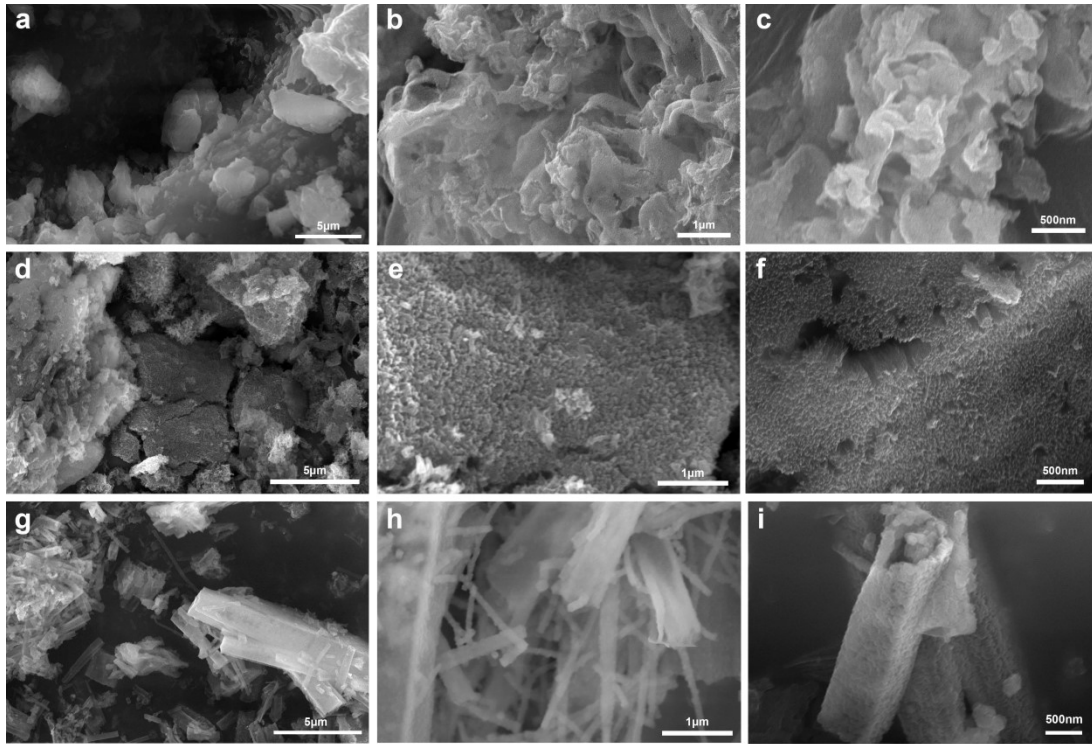
Fig. S1. SEM images of Melon (a, b, c), PHI (d, e, f) and PTI (g, h, i) at different magnifications.
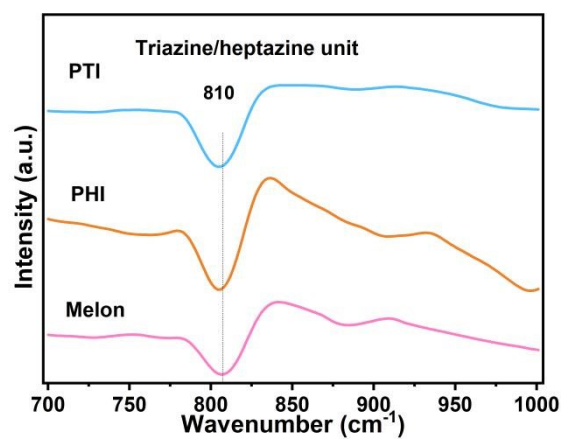
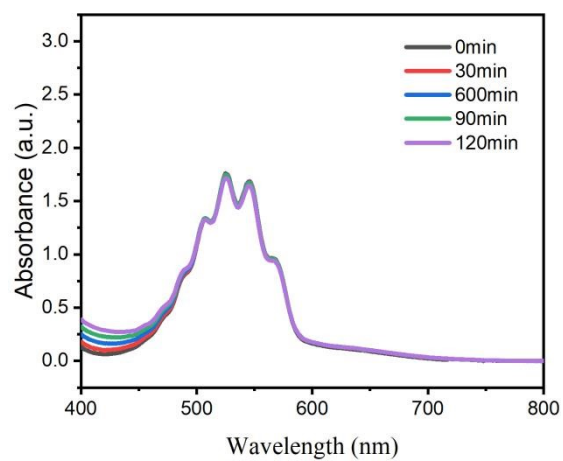**Fig. S2.** Amplified Fourier Transform infrared spectra for Melon, PHI and PTI.

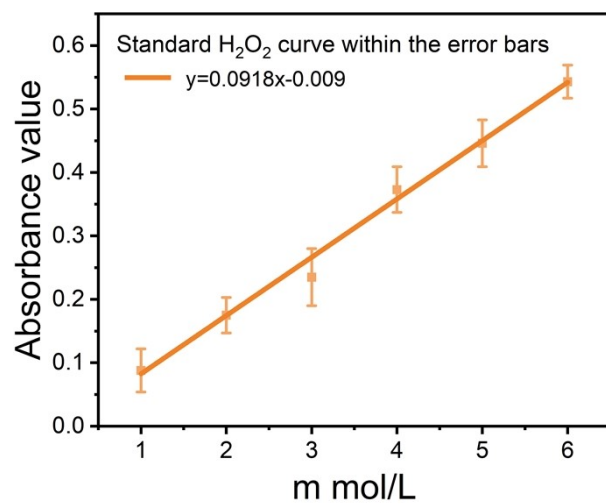**Fig. S3.** The absorbance of KMnO$_4$ solution under ultrasonication without catalysts.

Fig. S4. Standard conversion curve obtained by calibrating hydrogen peroxide normative solution.
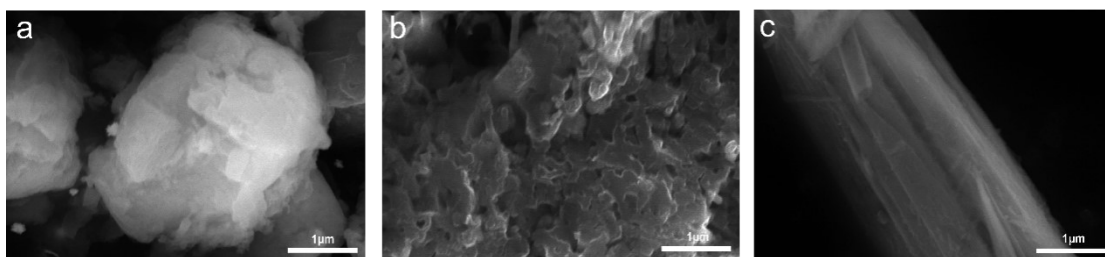
Fig. S5. SEM images of gold deposited (a) Melon, (b) PHI and (C) PTI taken by secondary electron mode.
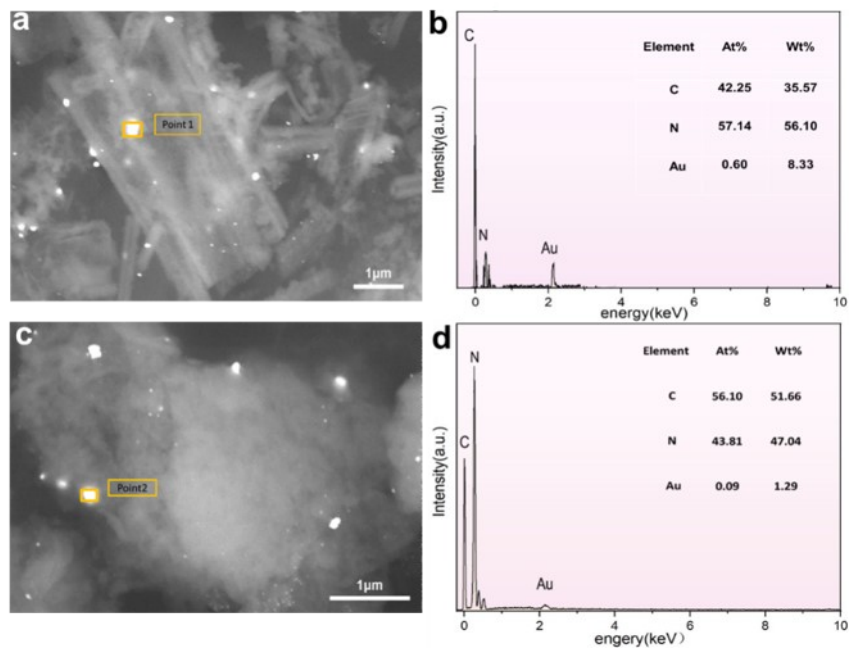
Fig. S6. The Energy Dispersive Spectroscopy (EDS) of Au deposition by point analysis. (a, b) PTI and (c, d) Melon. The content of Au element in PTI is more than that in Melon.
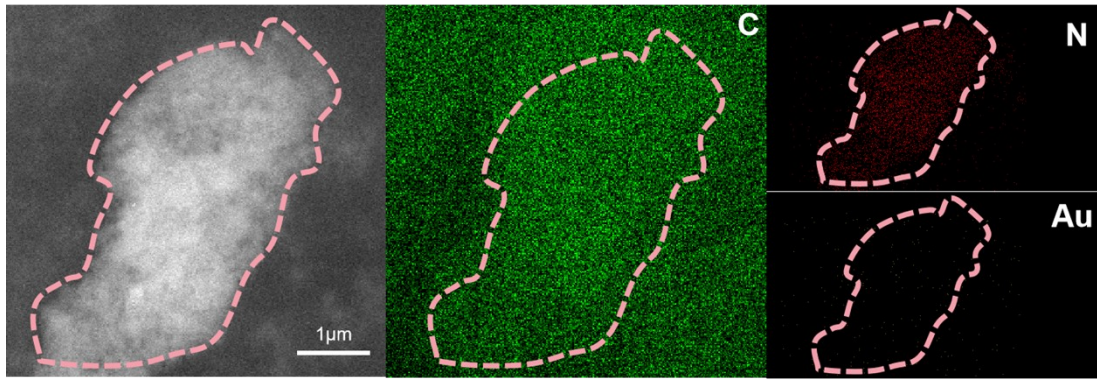
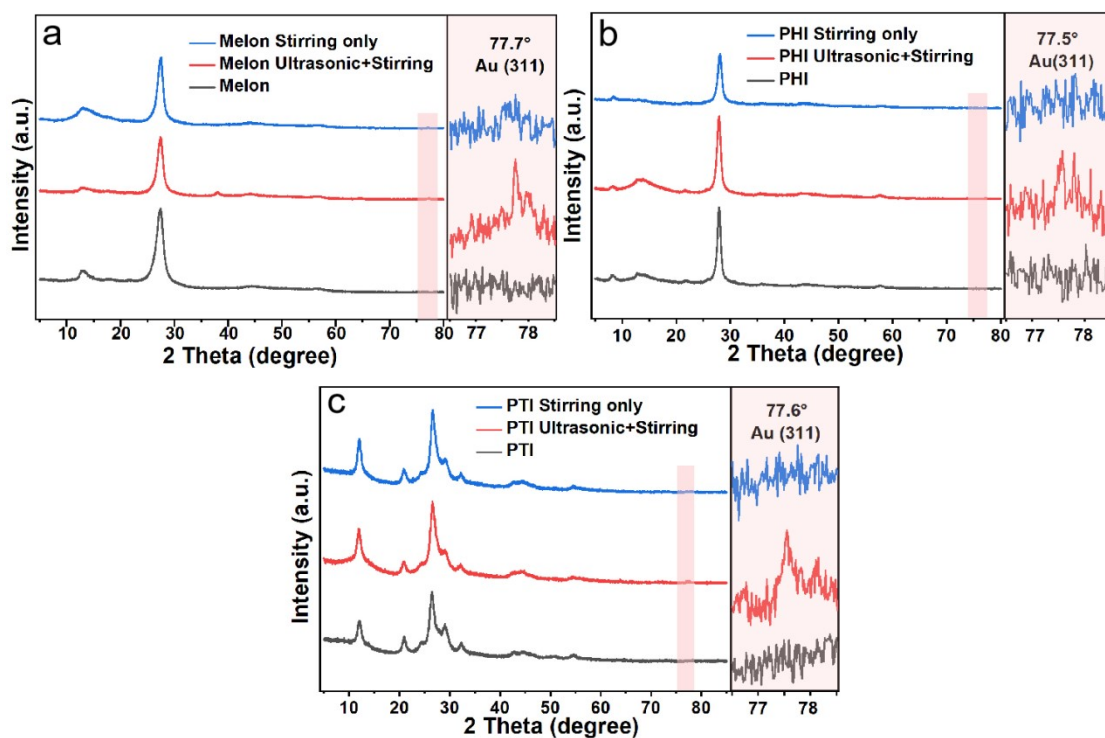**Fig. S7.** The Energy Dispersive Spectroscopy (EDS) mapping of Au deposited PHI.

Fig. S8. The XRD patterns of pristine and Au deposited (a) Melon, (b) PHI and (c) PTI, with the enlarged diffraction peaks of Au at around 77.5°.
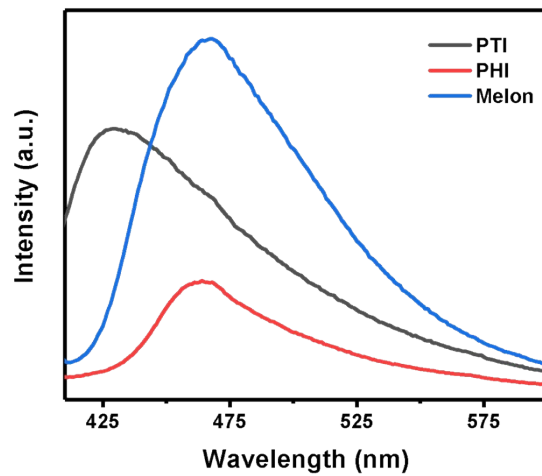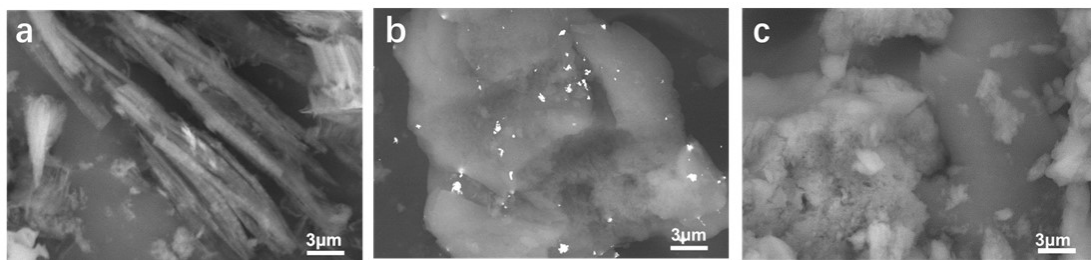
Fig. S9. Fluorescence emission spectra of samples.

Fig. S10. SEM observation of in-situ Au photo-deposition on (a) PTI, (b) PHI, (c) Melon in backscattered electron mode.
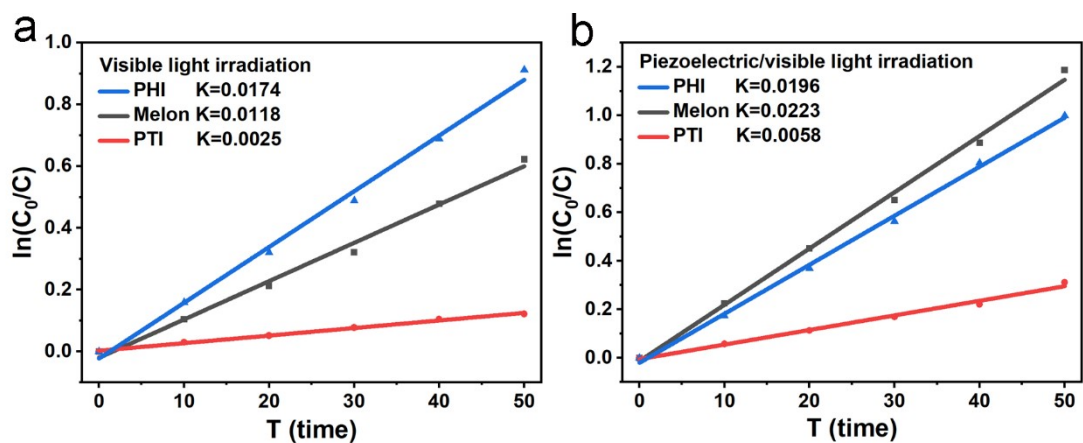
Fig. S11. The photocatalytic performances of RhB degradation for Melon, PHI and PTI under (a) visible light irradiation and (b) piezoelectric/visible light irradiation.

Table S1. FWHM of the characteristic peaks in XRD for different samples.

Samples	2-Theta	FWHM
Melon	13.173	0.792
Melon	27.734	0.667
PHI	8.113	0.627
PHI	28.205	0.587

Table S2. The pore information of Melon, PHI, PTI.

Samples	V_{pore} (cm^3 g^{-1})	APS$_{meso}$ (nm)
Melon	0.039	9.27
PHI	0.137	10.38
PTI	0.086	8.80

V_{pore} is the total pore volume and APS$_{meso}$ is the average mesopores size.

Reference:

1   Y. Feng, L. Ling, Y. Wang, Z. Xu, F. Cao, H. Li and Z. Bian, *Nano Energy* 2017, **40**, 481-486.